Kidney & Blood Pressure Research

Kidney Blood Press Res 2017;42:16-32
DOI: 10.1159/000464317
Published online: February 28, 2017
Accepted: December 21, 2016

Original Paper

Microarray Analysis Reveals Increased Expression of Matrix Metalloproteases and Cytokines of Interleukin-20 Subfamily in the Kidneys of Neonate Rats Underwent Unilateral Ureteral Obstruction: A Potential Role of IL-24 in the Regulation of Inflammation and Tissue Remodeling

Domonkos Pap[a,b] Erna Sziksz[a,b] Zoltán Kiss[b] Réka Rokonay[b]
Apor Veres-Székely[a,b] Rita Lippai[b] István Márton Takács[b] Éva Kis[a]
Andrea Fekete[c] György Reusz[b] Attila J. Szabó[a,b] Ádám Vannay[a,b]

[a]MTA-SE, Pediatrics and Nephrology Research Group; [b]1st Department of Pediatrics, Semmelweis University; [c]MTA-SE, Lendület Diabetes Research Group, Budapest, Hungary

Key Words
Newborn • Congenital obstructive nephropathy • Unilateral ureteral obstruction • CKD • Microarray • MMP-12, IL-24

Abstract
Background/Aims: Congenital obstructive nephropathy (CON) is the main cause of pediatric chronic kidney diseases leading to renal fibrosis. High morbidity and limited treatment opportunities of CON urge the better understanding of the underlying molecular mechanisms. ***Methods:*** To identify the differentially expressed genes, microarray analysis was performed on the kidney samples of neonatal rats underwent unilateral ureteral obstruction (UUO). Microarray results were then validated by real-time RT-PCR and bioinformatics analysis was carried out to identify the relevant genes, functional groups and pathways involved in the pathomechanism of CON. Renal expression of matrix metalloproteinase (MMP)-12 and interleukin (IL)-24 were evaluated by real-time RT-PCR, flow cytometry and immunohistochemical analysis. Effect of the main profibrotic factors on the expression of MMP-12 and IL-24 was investigated on HK-2 and HEK-293 cell lines. Finally, the effect of IL-24 treatment on the expression of pro-inflammatory cytokines and MMPs were tested *in vitro*. ***Results:*** Microarray analysis revealed

Ádám Vannay, MD, Ph.D.

1st Department of Pediatrics, Semmelweis University, H-1083 Budapest, Bókay J. u. 53-54 (Hungary), Tel. +36-1-3343186, Fax +36-1-3138212
E-Mail vannay.adam@med.semmelweis-univ.hu

880 transcripts showing >2.0-fold change following UUO, enriched mainly in immune response related processes. The most up-regulated genes were MMPs and members of IL-20 cytokine subfamily, including MMP-3, MMP-7, MMP-12, IL-19 and IL-24. We found that while TGF-β treatment inhibits the expression of MMP-12 and IL-24, H_2O_2 or PDGF-B treatment induce the epithelial expression of MMP-12. We demonstrated that IL-24 treatment decreases the expression of IL-6 and MMP-3 in the renal epithelial cells. **Conclusions:** This study provides an extensive view of UUO induced changes in the gene expression profile of the developing kidney and describes novel molecules, which may play significant role in the pathomechanism of CON.

Introduction

The most common cause of chronic kidney disease (CKD) in infants and children is congenital obstructive nephropathy (CON) characterized by renal tubular dilatation and parenchymal damage [1]. The severe form of CON is a progressive disease leading to markedly decreased renal function and finally to renal replacement therapy or transplantation. Although CON is a common disorder, its pathophysiology remains poorly understood and the underlying molecular mechanisms need to be elucidated.

Previous microarray studies performed on the kidney newborn rats revealed that ureteral obstruction activated the renin-angiotensin system (RAS), induced renal infiltration of neutrophils and macrophages and promoted the expression of immune modulator and structure genes [2, 3]. These processes lead to overproduction of reactive oxygen species [4, 5] and enhanced production of pro-inflammatory and profibrotic cytokines and growth factors, including interleukin (IL)-1β, IL-6, tumor necrosis factor (TNF)-α, transforming growth factor (TGF) -β or platelet derived growth factor (PDGF)-B [6-9]. These factors implicated in the progression of chronic inflammation and in the increased production of collagen-rich extracellular matrix (ECM) leading to fibrosis and CKD [10].

Although similar processes are observed in adult rats, there are certain distinctions. While inhibition of endogenous RAS is the primary intervention point in adults to slow down the progression of CKD, RAS inhibitors aggravate renal injury in the developing kidney of neonates [11, 12]. Similarly, although inhibition of TGF-β signaling pathway has beneficial effects in adult mice, it exacerbates renal injury in neonatal ones [13].

In the present study microarray analysis was performed to identify novel genes and molecular pathways involved in the pathomechanism of neonatal UUO-induced renal damage. Bioinformatics analysis was carried out to assess the main functional groups and pathways altered by differentially expressed genes derived from the microarray experiments. Based on the microarray results, we investigated the factors responsible for the expression of MMP-12 and IL-24 and also the biological role of IL-24 in the pathomechanism of CON. Our findings may contribute to the deeper understanding of molecular mechanisms of CON facilitating the identification of potential new therapeutic targets.

Materials and Methods

Animal model

The institutional committee on animal welfare approved all experiments (PEI/OO1/83-4/2013). Wistar rats (Charles River Laboratories, Sulzfeld, Germany) were housed in a temperature-controlled (22 ± 1 °C) room with 12-hour light and dark cycles cycles and mothers of the pups had free access to a standard rat chow and water. Newborn rats were randomly divided into two groups (N=6/group). Under general anaesthesia induced by inhalation of isoflurane mixed with air using a vaporizer (Eickemeyer Veterinary Equipment Ltd., Twickenham, UK) standard midline laparotomy was performed, and the bowel was gently

displaced from the abdomen. Then the left ureter was isolated by blunt dissection and completely ligated using fine suture material (UUO group). The bowel was then laid back and the muscle and skin were closed with nylon sutures. Sham-operated control animals underwent identical surgical procedure without occlusion of the left ureter (control group). Ten days after the initiation of UUO left kidneys were surgically removed. Kidney segments were fixed in 4% buffered formaldehyde immediately or snap-frozen in liquid nitrogen for the further molecular biological measurements.

Histological analysis

Paraffin sections of kidneys fixed in paraformaldehyde (4%, pH 7.4) were stained with Periodic acid-Schiff (PAS) reagents counterstained with haematoxylin eosin. Furthermore, Masson's trichrome staining was performed to evaluate the collagen deposition in the kidneys as one of main histological hallmarks of interstitial fibrosis. Images were taken with a Zeiss AxioImager A1 Light Microscope (Carl Zeiss GmbH, Jena, Germany) under 200x magnification from each kidney cross-sections with Pannoramic Viewer.

In vitro experiments

Human embryonic kidney (HEK-293) and human proximal tubular epithelial (HK-2) cell lines (American Type Culture Collection, Manassas, VA, USA) were cultured in Dulbecco's modified Eagle's medium (Gibco, Life Technologies, Carlsbad, CA, USA) supplemented with 10% fetal bovine serum (FBS) (Gibco, Life Technologies, Carlsbad, CA, USA) and 1% Penicillin-Streptomycin Solution (Sigma-Aldrich Co., St. Louis, MO, USA) in humidified 95% air and 5% CO_2 at 37°C. Cells with 70–80% confluency and between 6 and 10 passages were used for the *in vitro* experiments. HEK-293 and HK-2 cells were plated into 6-well tissue culture dishes ($5x10^5$ cells/well) (Sarstedt, Nümbrecht, Germany) than incubated in serum-free medium for 24 hours. Cells were treated either with 1nM recombinant human (rh) rhTGF-β or 0.4 nM rhPDGF-B or 2 nM rhIL-24 (R&D Systems, Minneapolis, MN, USA) or 25 μM H_2O_2 for 24 hours (N=6 well/treatment group). Control cells were treated with vehicle only. Then cells were trypsinised, centrifuged and pellets were collected for RT-PCR measurements.

RNA isolation and quality determination

Total RNA was isolated from frozen kidney samples and also from the HEK-293 and HK-2 cells by RNeasy RNA isolation kit according to the instructions of the manufacturer (Qiagen GmbH, Hilden, Germany). The quality and quantity of total RNA were determined with an Agilent 2100 Bioanalyser (Agilent Technologies, Palo Alto, CA, USA) then run on a 1% agarose gel. The same RNA samples over integrity score of 8.0 with a clear gel image without DNA contamination were used for the microarray and for the real-time RT-PCR measurements.

Microarray measurement

One-one μg RNA isolated from the kidney samples of newborn rats in the UUO (n=4) and control (n=3) groups was reverse transcribed by Low-input RNA Linear Amplification Kit (Agilent Technologies, Palo Alto, CA, USA) and then transcribed to Cy3-labeled complimentary RNA according to the manufacturer as described before [14]. After purification, the dye content (>9.0 pmol dye/μg cRNA) and concentration of cRNA was measured by NanoDrop ND-1000 spectrophotometer (NanoDrop Technologies, Wilmington, DE, USA). 825 ng of Cy3-labeled cRNA were mixed and hybridized to Whole Rat Genome Oligo 4x44k microarrays overnight. Then the slides were washed and treated with Stabilizing and Drying Solution and scanned by an Agilent Microarray Scanner (Agilent Technologies, Palo Alto, CA, USA). After normalization by the Feature Extraction software version 7.5 with default parameter settings for one-colour oligonucleotide microarrays, data were transferred to GeneSpring 9.02 program (Agilent Technologies, Palo Alto, CA) for further statistical evaluation. In GeneSpring the normalization and data transformation steps recommended by Agilent Technologies for one-colour data were applied. Genes with more than 2.0-fold differential expression were further analysed by statistical tests.

Real-time reverse transcription polymerase chain reaction (RT-PCR)

One μg RNA was reverse-transcribed using SuperScript III reverse transcriptase (Life Technologies, Carlsbad, CA, USA) to generate first-strand cDNA. The real-time RT-PCRs were performed in a final vol-

ume of 20 µl containing 0,5 µM of forward and reverse primers (Integrated DNA Technologies, Coralville, Iowa, USA), 10 µl of Light Cycler 480 SYBR Green I Master enzyme mix (Roche Diagnostics, Mannheim, Germany) and 1 µl cDNA on a LightCycler 480 system (Roche Diagnostics, Mannheim, Germany). The nucleotide sequences of the applied primer pairs, their specific optimal annealing temperatures and product lengths are summarized in Table 1. Results were analysed by Light-Cycler 480 software version 1.5.0.39 (Roche Diagnostics, Mannheim, Germany). mRNA expressions were normalized to the mRNA level of glyceraldehyde-3-phosphate dehydrogenase (GAPDH).

Table 1. Main technical data of the applied primer pairs. Summary of the nucleotide sequences and optimal annealing temperatures (T_a) of forward (F) and reverse (R) pairs applied in the real-time RT-PCRs of the study and also the length of the resulted products.

Name	Species	Primer pairs	Product length	T_a
MMP-3	rat	F: 5' -CCC TGA GCC TGG CTT TTA TTT GA -3' R: 5' -CAG GGA GGC CCA GAG TGT GAA- 3'	185 bp	57°C
MMP-7	rat	F: 5' -GGG AAC AGG CGC AGA ATT ATC TTA -3' R: 5' -ACA CCT GGG CTT CTG CAT TAT CTC -3'	167 bp	57°C
MMP-12	rat	F: 5' -ATG AAG CGT GCG GAT GTA GAC T -3' R: 5' -GAA ATG TGT TGG GGT GAA GGT ATC -3'	373 bp	56°C
IL-19	rat	F: 5' -AGT TGG CGA TTC TGC TGA TTC TCC -3' R: 5' -TTC TGT GGA CAT GCG CCT CCT G -3'	239 bp	57°C
IL-24	rat	F: 5' -AAG TGT CCG GCT GTT GAA -3' R: 5' -AGC ATG GCA TTG TCC TTA CT -3'	219 bp	52°C
IL-1ß	rat	F: 5'-GCA CTG CAG GCT TCG AGA TGA -3' R: 5'-GGT GGG TGT GCC GTC TTT CA -3'	220 bp	60°C
Clusterin	rat	F: 5'-GAA ATG AAG CTG AAG GCT TTC CCG -3' R: 5'-GGA ACT GTA AAG CTG GGC TAT GGA -3'	535 bp	60°C
Renin	rat	F: 5'-TGC CCA CCC TCC CCG ACA TT -3' R: 5'-GGC ACC CAG GAC CCA GAC AGG -3'	167 bp	60°C
GAPDH	rat	F: 5'-GGT GAA GGT CGG AGT CAA CG -3' R: 5'-CAA AGT TGT CAT GGA TGA CC -3'	159 bp	60°C
MMP-3	human	F: 5'-GGC AGT TTT GCT CAG CCT ATC CAT -3' R: 5'-TCC CCG TCA CCT CCA ATC CA -3'	197 bp	58°C
MMP-7	human	F: 5' -GTG GGA ACA GGC TCA GGA CTA TC -3' R: 5' -ACA TCT GGG CTT CTG CAT TAT TTC -3'	169 bp	55°C
MMP-12	human	F: 5'-CTG GTT CTG AAT TGT CAG GAT -3' R: 5'-ACA TTT CGC CTC TCT CTG C -3'	99 bp	60°C
IL-1β	human	F: 5' -CAC GCT CCG GGA CTC ACA G -3' R: 5' -GCC CAA GGC CCA CAG GTA TTT T -3'	160 bp	56°C
IL-6	human	F: 5' -AAAGATGGCTGAAAAAGATGGAT-3' R: 5' -CTCTGGCTTGTTCCTCACTACTCT-3'	146 bp	60°C
TNF-α	human	F: 5' -GAGGCGCTCCCCAAGAAGACA-3' R: 5' -TGGGCCAGAGGGCTGATTAGAG -3'	182 bp	61°C
IL-24	human	F: 5' -AGG CGG TTT CTG CTA TTC C -3' R: 5' -GAG CTG CTT CTA CGT CCA ACT -3'	55 bp	48°C
GAPDH	human	F: 5' -AGC AAT GCC TCC TGC ACC ACC AA-3' R: 5' -GCG GCC ATC ACG CCA CAG TTT-3'	159 bp	60°C

Gene ontology (GO) term analysis

As the first stage of bioinformatics analysis we assessed the main functional groups of the differentially expressed genes derived from the microarray experiments. Therefore we performed GO term analysis in all domains of ontology on the dysregulated genes using the Database for Annotation, Visualization and Integrated Discovery (DAVID, https://david.ncifcrf.gov) [15, 16]. GO terms for the species Rattus norvegicus were included in the analysis. We used Fisher's exact test to conduct an enrichment analysis with 0.05 threshold for the p-values of enriched categories adjusted with the Benjamini-Hochberg correction method. To reduce the biologicaly unsignificant hits we tested 10 size-matched random draws from the Rattus norvegicus genome. Cytoscape software (http://www.cytoscape.org) was used to visualize the results on a network graph.

Reactome pathway analysis

Transcript ID-s of differentially expressed mRNAs were mapped to UniProt protein ID-s in order to form a potential pool of altered proteins. The resulting list was transferred to the Reactome Pathway Database (http://www.reactome.org) [17]. In Reactome, protein homology data were obtained from Ensmbl Compara database, which created a homology-based inference in the human proteome [18]. This method allowed to find interactions and pathways which are similar in species Rattus norvegicus and Homo sapiens. On the resulting pathway overrepresentation analysis a Fisher's exact test adjusted with the Benjamini-Hochberg correction method was carried out. All related pathway mappings were then extracted and mapped on pathways after a FDR cutoff of 0.05. The resulting pathway involvement network was visualized in the Cytoscape software (http://www.cytoscape.org) [19].

Flow cytometry

After 10 days of UUO, kidneys were harvested, and the tissue was homogenized by collagenase II (Sigma-Aldrich, St. Louis, MO) to generate single cell suspension. Cell pellets were incubated with Fixation/Permeabilization solution (BD Bioscience Co., California, USA) for 10 min at RT. After permeabilization, cells were washed with Perm/Wash™ Buffer (BD Bioscience Co., California, USA) and incubated with IL-24 specific (rabbit monoclonal IgG, Abcam, Cambridge, UK) and MMP-12 specific (goat polyclonal IgG, Santa Cruz Biotechnology Inc., Dallas, TX) antibody diluted to 1:50 for 30 min at RT. Cells were subsequently washed with Perm/Wash™ Buffer and incubated with secondary antibodies ((Alexa Fluor 488 chicken anti-rabbit IgG, and Alexa Fluor 647 donkey anti-goat IgG (Invitrogen, Life Technologies, Carlsbad, CA, USA)) diluted to 1:50 for 30 min, at RT, in the dark. Appropriate controls were performed omitting the primary antibodies to assure their specificity and to avoid autofluorescence. Thereafter cells were washed with Perm/Wash™ Buffer, and resuspended in PBS. The flow cytometric analysis was carried out using a FACSAria cytometer (BectonDickinson, San Jose, CA, USA). According to the forward and side scatter, we identified an intact cell gate (without debris). Ten thousand cells were collected and results were analysed using the BD FACSDiva Software (BectonDickinson, San Jose, CA, USA).

Immunohistochemical analysis

Immunohistochemistry was performed on paraffin-embedded 5 μm thick tissue sections fixed in formalin (4%, pH 7.4). Slides were deparaffinized in xylene, rehydrated in graded ethanol series, and washed in distilled water. Heat induced epitope retrieval was performed by boiling the tissue sections in citrate buffer (HISTOLS® -Citrate Buffer, pH 6.0; Histopathology, Ltd.) in a microwave oven at 750 W for 15 minutes, followed by cooling at room temperature for 20 minutes. Slides were washed in TBS. Nonspecific sites were blocked (HISTOLS® Background Blocking Protein Solution, cat#30013, Histopathology, Ltd.) for 10 minutes at room temperature. Without washing, the following primary antibodies were applied: anti-MMP-12 (rabbit monoclonal IgG, Abcam, Cambridge, UK) in 1:100 dilution and anti-IL-24 (rabbit monoclonal IgG, Abcam, Cambridge, UK) in 1:50 dilution. Incubation with the primary antibodies was performed for 1 hour at room temperature followed by repeated washing in TBS. Secondary antibody (HISTOLS® -R anti-rabbit Detection Systems (cat# 30011R, Histopathology, Ltd.) was applied for 30 minutes at room temperature followed by repeated washing in TBS. Sections were incubated with 3,3'-Diaminobenzidine (HISTOLS® -DAB chromogen/Substrate System, cat#30014.K, Histopathology, Ltd.), washed in distilled water, counter stained with haematoxylin followed by washing in tap water. For the negative control antibody diluent without primary antibody was used before the application of the secondary antibody. Sections were then dehydrated, cleared in xylene and mounted with permanent mounting medium.

Fluorescent immunohistochemistry

IL-24 has two heterodimer cell surface receptors (IL-20Rα/IL-20Rβ and the IL-22Rα/IL-20Rβ) both containing the inducible IL-20Rβ subunit. Here we investigated the presence of IL-20Rβ on the HEK-293 and HK2 cells cultured in tissue culture chambers (Sarstedt Kft., Budapest, Hungary). After repeated washing, the cells were fixed in 4% paraformaldehyde, washed again, and permeabilized with Triton X-100 (Sigma-Aldrich). Cells were incubated with anti-IL-20Rβ (rabbit monoclonal IgG, Abcam, Cambridge, UK). After repeated washing, the chambers were incubated with anti–rabbit Alexa Fluor 568 conjugate secondary antibody and counterstained with Hoechst 33342. Appropriate controls were performed by omitting the primary antibody to assure the specificity and avoid autofluorescence. Sections were analysed with a Zeiss LSM 510 Meta Confocal Laser-Scanning Microscope (Carl Zeiss GmbH) with objectives of magnification ×400.

Statistical analysis

The statistical evaluation of real-time RT-PCR and flow cytometric results were performed by GraphPad Prism 6.01 software (GraphPad Software Inc., La Jolla, CA, USA). After testing normality with Kolmogorov-Smirnov test Mann–Whitney U-test or unpaired, two-tailed t-test was used to determine the differences between two groups. $p \leq 0.05$ was considered as statistically significant. Values were expressed as mean+SD.

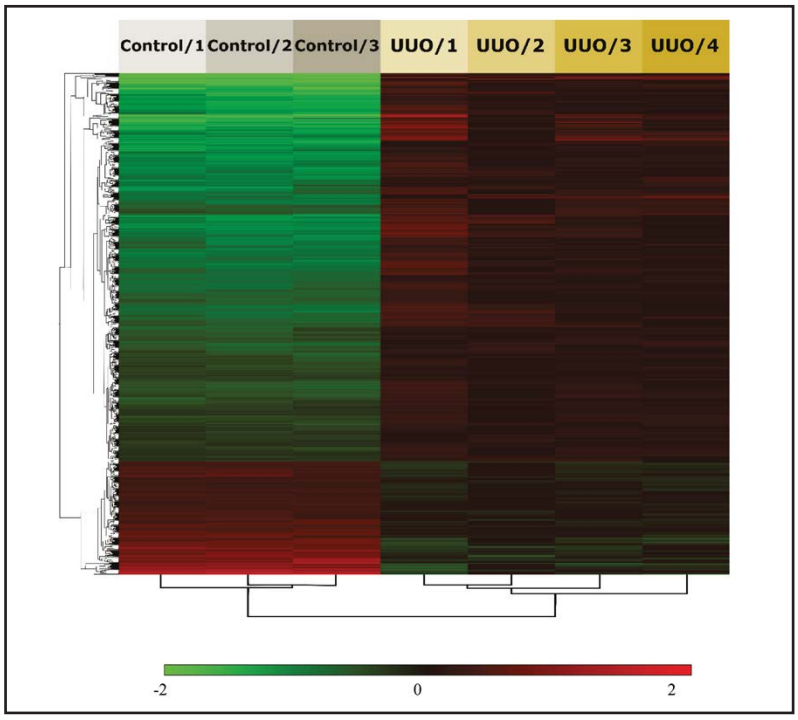

Fig. 1. Clustered heat map of the differentially expressed genes in control and obstructed kidneys. Expression of 681 genes was upregulated and 199 genes were downregulated in kidneys of sham-operated control and ureteral obstructed mice (fold change> |2|; $p<0.05$). Green and red colors denote the significantly increased or decreased genes. Dendrograms show hierarchical clustering of differentially expressed genes.

Results

UUO-induced histological changes in the kidney

PAS and Masson's trichrome staining of control kidneys revealed normal kidney structure, without glomerular, tubular or interstitial lesions. On the contrary, severe pathological changes in the tubulointerstitium characterized by parenchymal damage, tubular atrophy and dilatation with widened interstitial spaces were observed in kidneys underwent UUO. Masson's trichrome staining revealed unequivocal signs of increased collagen deposition in the kidney of newborn rats underwent UUO compared to that of sham-operated controls (Figure 2).

Microarray results

Microarray analysis of the RNA samples isolated from the kidneys of newborn rats using a whole rat genome microarray kit revealed a marked change in the gene expression profile after 10 days of UUO compared to sham-operated controls (ArrayExpress: E-MTAB-4984). Eight hundred and eighty transcripts showed >2.0 fold, statistically significant alterations following UUO. Among them 681 transcripts were significantly upregulated and 199 transcripts were markedly downregulated as a consequence of UUO-induced renal injury (Figure 1 and Supplemental Table 1).

All supplementary materials are linked to the online version of the paper at http://www.gyermekklinika.semmelweis.hu/info.aspx?sp=123.

The significantly altered transcripts were then sorted into a list based on their gene expressional fold change values. The first 10 genes with the highest and lowest fold change are shown in Table 2.

Results of GO term analysis

The initial DAVID-based GO term analysis of the differentially expressed genes following UUO resulted in 81 GO terms in the biological function (Supplemental Figure 1 and Supplemental Table 2), 13 GO terms in the molecular function (Supplemental Table 3) and

20 GO terms in the cellular localization (Supplemental Table 4) domain. The 10 most abundant categories of the domains are summarized in Table 3.

Results of Reactome pathway analysis

Enrichment analysis using Reactome Pathway Database identified 86 over-represented pathways summarized in Supplemental Table 5. Based on the number of entities the 10 major pathways were as follows: Innate Immune System, Cytokine Signaling in Immune system, Adaptive Immune System, GPCR ligand binding, Class A/1 Rhodopsin-like receptors, Signaling by Interleukins, Peptide ligand-binding receptors, G alpha (i) signaling events, Platelet activation, signaling and aggregation, Toll-Like Receptors Cascades (Table 4 and Supplemental figure 2).

Renal expression of MMP-3, MMP-7, MMP-12, IL-1ß, IL-19, IL-24, renin and clusterin

To validate our microarray measurements real-time RT-PCRs were performed. Based on the microarray results eight genes were selected for validation. mRNA expression of

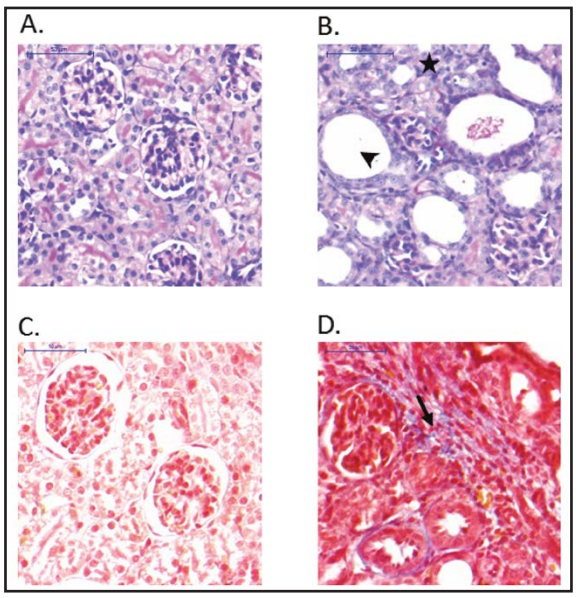

Fig. 2. Representative pictures of PAS (A, B) and Masson's trichrome (C, D) stained kidney sections of sham-operated control (A, C) and unilateral ureteral obstructed (UUO) newborn rats (B, D). Tubular atrophy (asterisk), dilatation (arrowhead) with widened interstitial spaces (B) and significant interstitial collagen deposition were present in the obstructed kidney samples (D; arrow). Original magnification, ×200. Scale bar, 50 µm.

Table 2. Genes with the highest and lowest fold change based on the microarray results. Table shows the mean intensity (MI) values and fold change (FC) of the expected and identified number of associated genes; p-p value (unpaired, two-tailed t-test); FDR-Multiple test correction controlled with the Bonferroni-Hochberg method.

Gene	Gene Name	Control MI	UUO MI	FC	p	FDR
Genes up-regulated in the kidney of neonatal rats underwent unilateral ureteral obstruction						
Mmp7	matrix metalloproteinase 7	-9.256	0.518	875.8	< 0.01	< 0.05
Mmp3	matrix metallopeptidase 3	-6.299	1.637	244.8	< 0.01	< 0.05
Trh	thyrotropin releasing hormone	-5.876	0.948	113.3	< 0.01	< 0.05
Aoc1	amiloride binding protein 1	-6.318	0.399	105.2	< 0.01	< 0.05
Il19	interleukin 19 (predicted)	-5.657	0.972	98.9	< 0.01	< 0.05
Mmp12	matrix metallopeptidase 12	-5.132	1.421	93.9	< 0.01	< 0.05
Dmbt1	deleted in malignant brain tumours 1	-6.272	0.234	90.9	< 0.01	< 0.05
Il24	interleukin 24	-6.039	0.455	90.1	< 0.01	< 0.05
Dio3	deiodinase, iodothyronine, type III	-5.912	0.560	88.7	< 0.01	< 0.05
C4bpa	complement component 4 binding protein, alpha	-4.622	1.241	58.2	< 0.01	< 0.05
Genes down-regulated in the kidney of neonatal rats underwent unilateral ureteral obstruction						
Pex5l	peroxin 2	3.287	-0.581	-14.6	< 0.01	< 0.05
Fmo3	flavin containing monooxygenase 3	2.961	-0.644	-12.2	< 0.01	< 0.05
Vwc2	von Willebrand factor C domain containing 2	2.879	-0.633	-11.4	< 0.01	< 0.05
Spna1_	spectrin alpha 1 (predicted)	2.981	-0.403	-10.4	< 0.01	< 0.05
Mlana	melan-A	2.540	-0.814	-10.2	< 0.01	< 0.05
Gcm1	glial cells missing homolog 1 (Drosophila)	2.155	-1.077	-9.4	< 0.01	< 0.05
Myh13	myosin, heavy polypeptide 13, skeletal muscle	2.418	-0.663	-8.5	< 0.01	< 0.05
Kcnj10	potassium inwardly-rectifying channel, subfamily J, member 10	2.325	-0.671	-8.0	< 0.01	< 0.05
Lrrc66	leucine rich repeat containing 66	2.038	-0.874	-7.5	< 0.01	0.05
Myh7	myosin, heavy polypeptide 7, cardiac muscle, beta	2.124	-0.791	-7.5	< 0.01	< 0.05

Table 3. List of the ten most abundant GO terms in the biological and molecular function and cellular localisation domain showing alteration in the kidney of newborn rats underwent UUO compared to those of controls. Abbreviations used in the letterhead: Count-number of entities associated with the term; Enrichment-ratio of the expected and identified number of associated genes; Occurance-occurance in random sets; p-p value calculated with Fisher's exact test; FDR-Multiple test correction controlled with the Bonferroni-Hochberg method.

GO terms	Co-unt	Enrich-ment	Occur-ence	p value	FDR
GO terms in the biological function domain					
immune response	47	6.651	0/10	< 0.01	< 0.01
inflammatory response	41	5.846	0/10	< 0.01	< 0.01
response to lipopolisacharide	34	4.757	0/10	< 0.01	< 0.01
innate immune response	32	5.040	0/10	< 0.01	< 0.01
response to drug	32	2.390	0/10	< 0.01	< 0.01
negative regulation of apoptotic process	30	2.227	0/10	< 0.01	< 0.01
response to hypoxia	27	3.939	0/10	< 0.01	< 0.01
positive regulation of cell proliferation	27	2.049	0/10	< 0.01	< 0.05
aging	25	3.158	0/10	< 0.01	< 0.01
cellular response to lipopolysaccharide	24	4.805	0/10	< 0.01	< 0.01
GO terms in the molecular function domain					
protein homodimerization activity	46	2.288	0/10	< 0.01	< 0.01
cytokine activity	18	4.620	0/10	< 0.01	< 0.01
protein binding	69	1.766	0/10	< 0.01	< 0.01
protease binding	13	4.798	0/10	< 0.01	< 0.01
cytokine receptor activity	8	9.395	0/10	< 0.01	< 0.01
chemokine activity	8	8.612	0/10	< 0.01	< 0.01
receptor binding	24	2.642	0/10	< 0.01	< 0.01
protein heterodimerization activity	30	2.149	0/10	< 0.01	< 0.05
tumor necrosis factor receptor binding	7	7.978	0/10	< 0.01	< 0.05
protein complex binding	22	2.395	0/10	< 0.01	< 0.05
GO terms in the cellular localization domain					
extracellular space	93	2.837	0/10	< 0.01	< 0.01
cell surface	60	3.816	0/10	< 0.01	< 0.01
external side of plasma membrane	33	4.773	1/10	< 0.01	< 0.01
membrane raft	27	3.996	0/10	< 0.01	< 0.01
extracellular region	43	2.350	1/10	< 0.01	< 0.01
MHC class II protein complex	7	19.018	0/10	< 0.01	< 0.01
extracellular matrix	19	4.083	0/10	< 0.01	< 0.01
blood microparticle	14	4.513	0/10	< 0.01	< 0.01
neuronal cell body	31	2.290	0/10	< 0.01	< 0.01
integral component of plasma membrane	40	1.956	0/10	< 0.01	< 0.01

Table 4. Major pathways identified by Reactome pathway analysis of the altered genes in the kidney of newborn rats following UUO. Abbreviations used in the letterhead: Ratio of protein- Ratio of protein in pathway; Number of protein-number of protein in pathway; Count-number of entities associated with the pathway; p-p value calculated with Fisher's exact test; FDR-Multiple test correction controlled with the Bonferroni-Hochberg method.

Reactome Pathway	Ratio of protein	Number of protein	Count	p	FDR
Innate Immune System	0.113	806	61	< 0.01	< 0.01
Cytokine Signaling in Immune system	0.069	489	44	< 0.01	< 0.01
Adaptive Immune System	0.086	609	37	< 0.01	0.053
GPCR ligand binding	0.055	389	30	< 0.01	< 0.01
Class A/1 (Rhodopsin-like receptors)	0.043	304	27	< 0.01	< 0.01
Signaling by Interleukins	0.039	280	25	< 0.01	< 0.01
Peptide ligand-binding receptors	0.027	191	20	< 0.01	< 0.01
G alpha (i) signaling events	0.030	212	20	< 0.01	< 0.05
Platelet activation, signaling and aggregation	0.029	203	19	< 0.01	< 0.05
Toll-Like Receptors Cascades	0.019	132	14	< 0.01	< 0.05

MMP-3 ($p<0.01$ vs. Control), MMP-7 ($p<0.01$ vs. Control), MMP-12 ($p<0.05$ vs. Control), IL-19 ($p<0.01$ vs. Control) and IL-24 ($p<0.01$ vs. Control) was studied as these genes showed the highest fold-change in our model (as shown in Table 1). Moreover, IL-1ß ($p<0.05$ vs. Control), renin ($p<0.05$ vs. Control) and clusterin ($p<0.05$ vs. Control) were selected for further validation as literally well-known regulators of UUO induced renal fibrosis [3]. In accordance with the results of our microarray analysis, we found significantly elevated mRNA expression of each genes selected for validation in the kidney of newborn rats after 10 days of UUO compared to sham-operated controls (Figure 3).

Renal level of MMP-12 and IL-24

To validate our microarray gene expression data at protein level flow cytometric measurements were performed. In accordance with the microarray and real-time RT-PCR results, higher protein level of MMP-12 and IL-24 were found in the kidneys of newborn rats

10 days after the onset of UUO compared to sham-operated control kidneys ($p<0.01$, respectively) (Figure 4).

Renal localization of MMP-12 and IL-24

MMP-12 immunopositivity was diffusely present in the cytoplasm of the tubular epithelial and glomerular cells of control and ureteral obstructed kidneys of the newborn rats in the renal cortex and medulla as well. All tubular segments were involved in the intraepithelial distribution of MMP-12. However, MMP-12 immunopositivity was more pronounced in the kidneys of newborn rats underwent UUO compared to controls (Figure 5/ A and B). In case of IL-24 staining renal tubular epithelial and glomerular cells showed immunopositivity in the renal cortex of newborn rats underwent UUO. In the kidneys of the control newborn rats IL-24 immunopositivity was not detectable (Figure 5/ C and D).

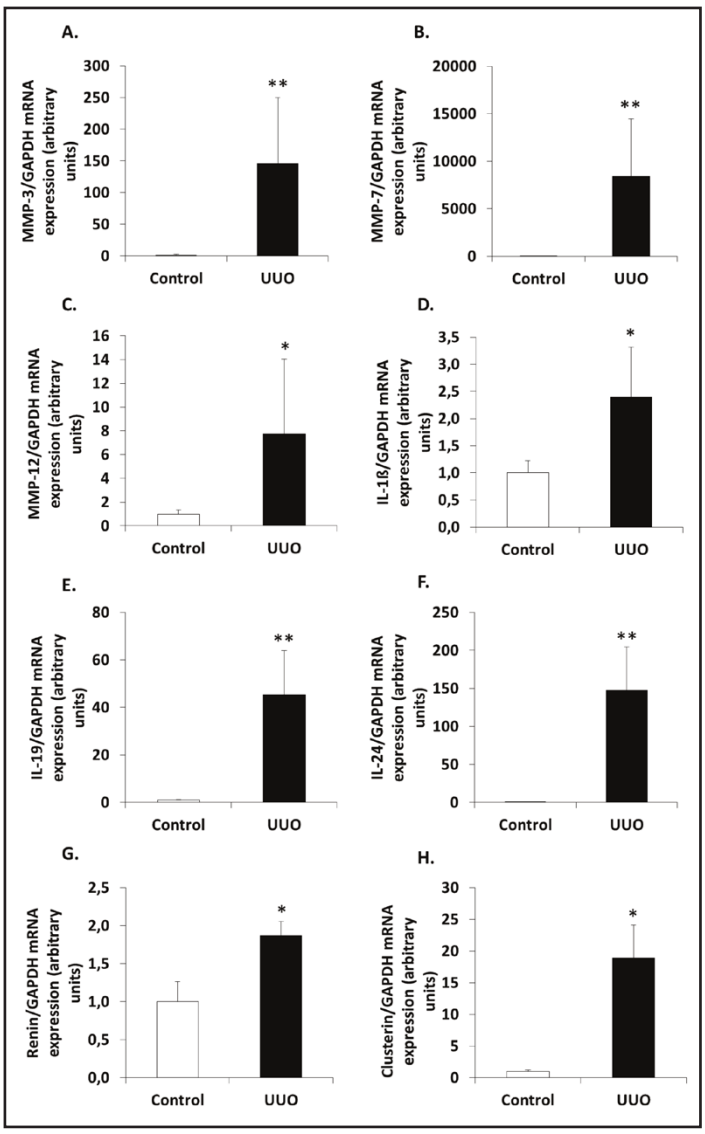

Fig. 3. Validation of the microarray results by RT-PCR: mRNA expression of metalloproteinase (MMP)-3, MMP-7, MMP-12 (A, B and C), interleukin (IL)-1ß, IL-19 IL-24 (D, E and F), renin (G) and clusterin (H). Increased mRNA expression of MMP-3, MMP-7, MMP-12 (A, B and C), IL-1ß, IL-19, IL-24 (D, E and F), renin (G) and clusterin (H) was found in the kidney of newborn rats underwent UUO compared to sham-operated control kidneys. Results are presented as mean+SD. *$p<0.05$ vs. Control, **$p<0.01$ vs. Control.

Effect of TGF-ß, PDGF-B or H_2O_2 treatment on the MMP-12 and IL-24 expression in embryonic kidney cells

The effect of 24h rhTGF-ß, rhPDGF-B or H_2O_2 treatment on the mRNA expression of MMP-12 and IL-24 was investigated in HEK-293 embryonic kidney cell line by RT-PCR. rhTGF-ß treatment significantly decreased the mRNA expression of MMP-12 and IL-24 compared to vehicle-treated controls ($p<0.05$, respectively). While administration of rhPDGF-B or H_2O_2 significantly increased the mRNA expression of MMP-12 ($p<0.05$ vs. Control), mRNA expression of IL-24 remained unchanged (Figure 6).

Effect of TGF-ß, PDGF-B and H_2O_2 on the MMP-12 and IL24 expression of human proximal tubular epithelial cells

To investigate the effect of 24h rhTGF-ß, rhPDGF-B and H_2O_2 treatment on the mRNA expression of MMP-12 and IL-24 in HK-2 human proximal tubular epithelial cell line, RT-PCRs

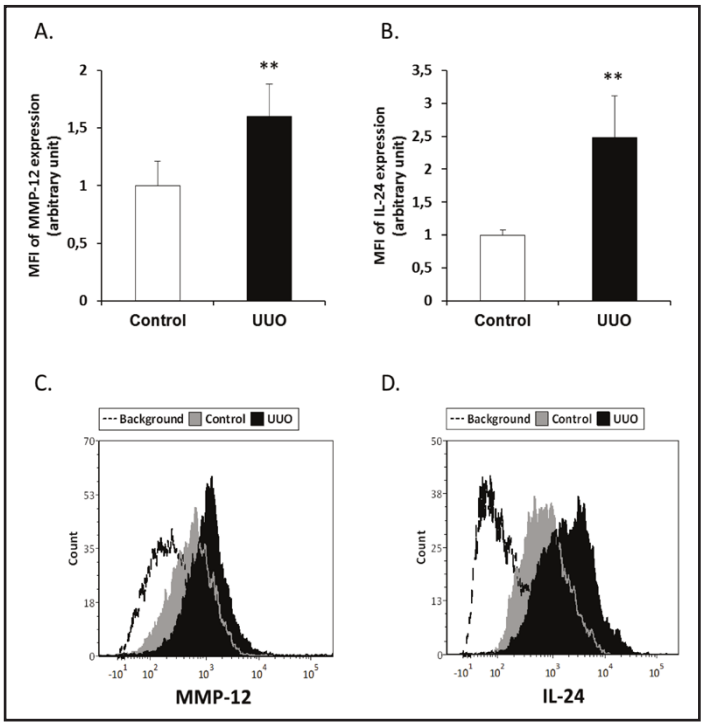

Fig. 4. Protein level of matrix metalloproteinase (MMP)-12 and interleukin (IL)-24 in the kidney of newborn rats 10 days after the onset of unilateral ureteral obstruction (UUO) or sham-operation. Increased protein level of MMP-12 (A) and IL-24 (B) were found in the kidney of newborn rats underwent UUO compared to sham-operated controls. The representative flow cytometric histograms show the changes in the level of MMP-12 (C) and IL-24 in the kidneys (D) following UUO. Results are presented as mean+SD. **p<0.01 vs. Control.

were performed. rhTGF-ß significantly decreased the mRNA expression of MMP-12 and IL-24 in HK-2 cells compared to vehicle-treated controls (p<0.05, respectively). Administration of rhPDGF-B had no effect on the MMP-12 or IL-24 expression in HK-2 cells. While treatment with H_2O_2 significantly increased the mRNA expression of MMP-12 (p<0.05 vs. Control) it did not alter the mRNA expression of IL-24 in HK-2 cells compared to vehicle-treated controls (Figure 7).

IL-20Rβ expression in human embryonic kidney and proximal tubular epithelial cells

To investigate the presence of IL-20Rβ on HEK-293 embryonic kidney and HK2 human renal tubular epithelial cells fluorescent immunohistochemical staining was performed. We found strong IL-20Rβ immunopositivity in HEK-293 and HK-2 cells as well. (Figure 8).

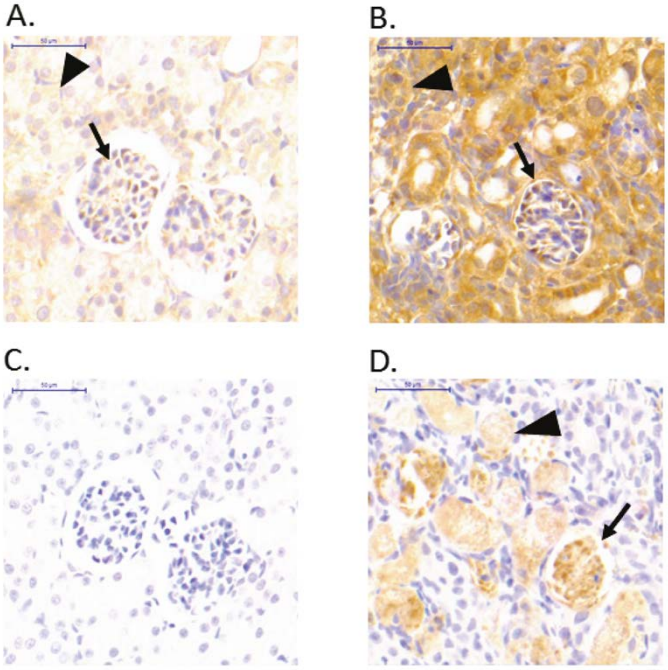

Fig. 5. Representative pictures of kidney sections of sham-operated control (A, C) and unilateral ureteral obstructed (UUO) newborn rats (B, D) stained with anti-metalloproteinase (MMP)-12 and anti-interleukin (IL)-24 monoclonal antibodies. Tubular epithelial (arrowheads) and glomerular cells (arrows) of control (A) and ureteral obstructed kidneys (B) show uniform staining for MMP-12. IL-24 immunopositivity was present only in the renal tubular epithelial (arrowheads) and glomerular cells (arrows) of rats underwent UUO (D). Original magnification, ×200. Scale bar, 50 µm.

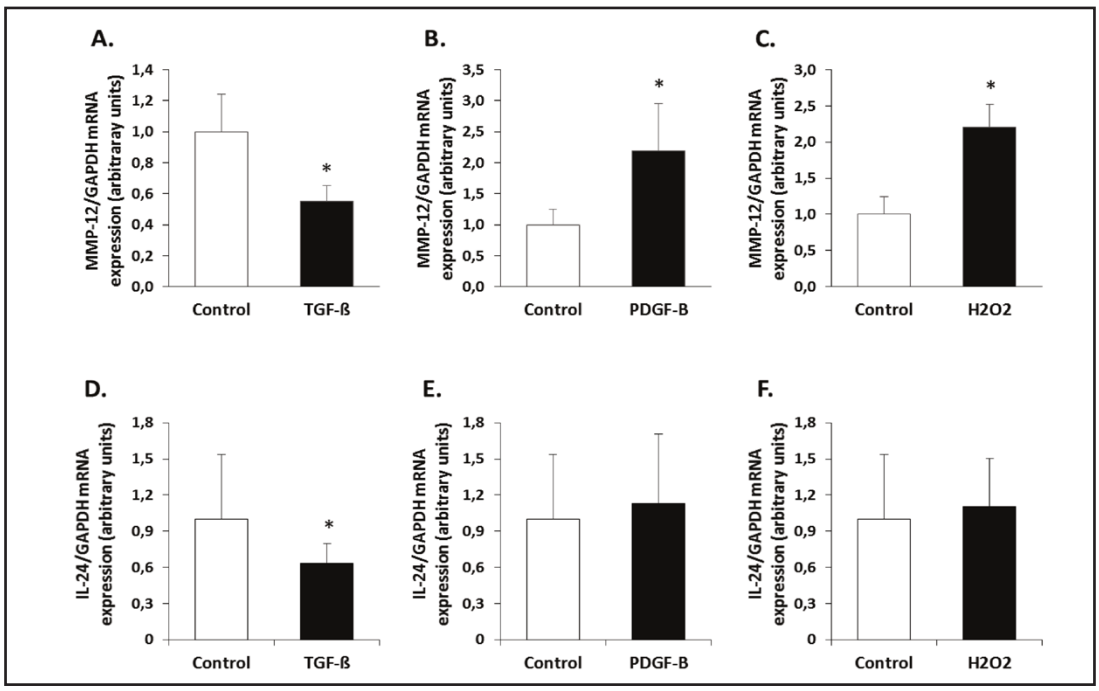

Fig. 6. Effect of transforming growth factor (TGF)-ß (A,D), platelet derived growth factor (PDGF)-B (B,E) and H_2O_2 (C,F) on the mRNA expression of matrix metalloproteinase (MMP)-12 and interleukin (IL)-24 in HEK-293 embryonic kidney cells. Results are presented as mean+SD. *p<0.05 vs. Control.

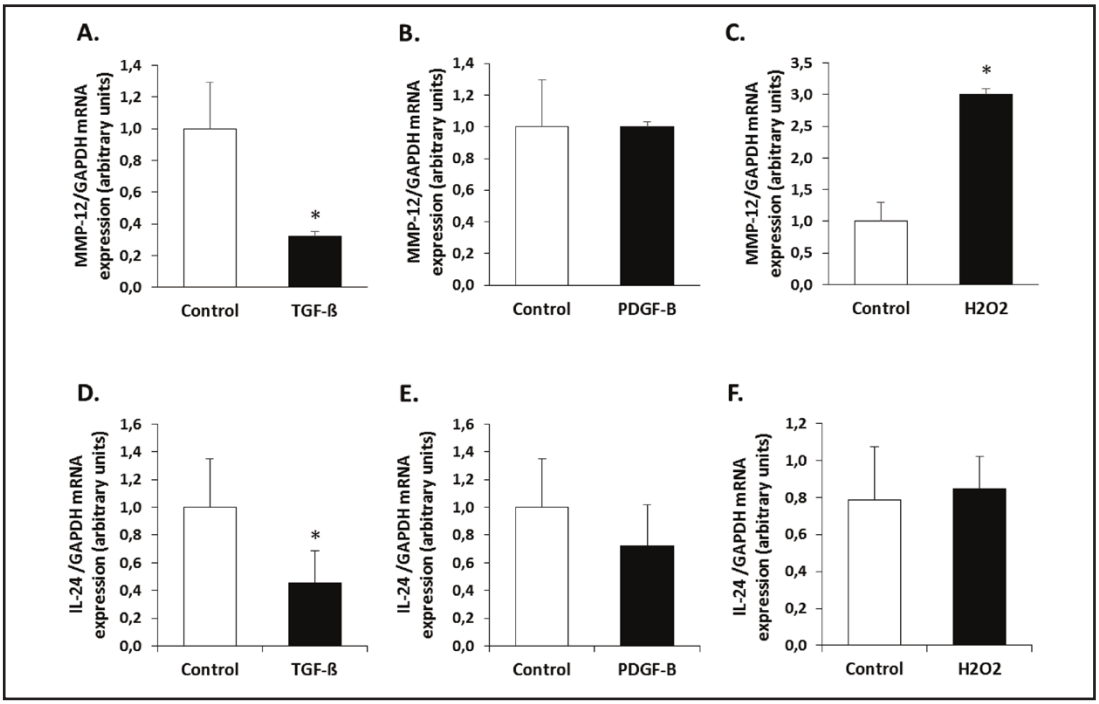

Fig. 7. Effect of transforming growth factor (TGF)-ß (A, D), platelet derived growth factor (PDGF)-B (B, E) and H_2O_2 (C, F) on the mRNA expression of matrix metalloproteinase (MMP)-12 and interleukin (IL)-24 in HK2 human renal tubular epithelial cells. Results are presented as mean+SD. *p<0.05 vs. Control.

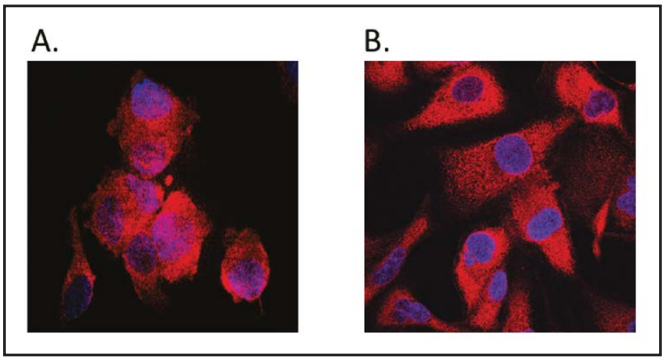

Fig. 8. Representative pictures of HEK-293 embryonic kidney cells (A) and HK2 human renal tubular epithelial cells (B) stained with anti-interleukin (IL)-20 receptor beta (Rβ) monoclonal antibodies. IL-20Rβ is stained with red, nuclei are stained with blue. Original magnification, ×400.

Effect of IL-24 treatment on the IL-1β, TNF-α, IL-6, MMP-3, MMP-7 and MMP-12 expression of embryonic kidney and human proximal tubular epithelial cells

The effect of 24h rhIL-24 treatment on the mRNA expression of pro-inflammatory cyto-kines (IL-1β, IL-6 and TNF-α) as well as MMPs (MMP-3, MMP-7 and MMP 12) was investigated in HEK-293 and HK2 cell lines by RT-PCR. rhIL-24 treatment significantly decreased the expression of IL-6 ($p<0.05$ vs. Control) in HEK-293 cells, but in the HK-2 cells it remained unchanged. rhIL-24 treatment also decreased the mRNA expression of MMP-3 ($p<0.05$ vs. Control) both in HEK-293 and HK-2 ($p<0.05$ vs. Control) (Figure 9) cells. The mRNA expression of IL-1β, TNF-α, MMP-7 or MMP-12 (data not shown) did not alter in the studied renal epithelial cell lines after rhIL-24 treatment.

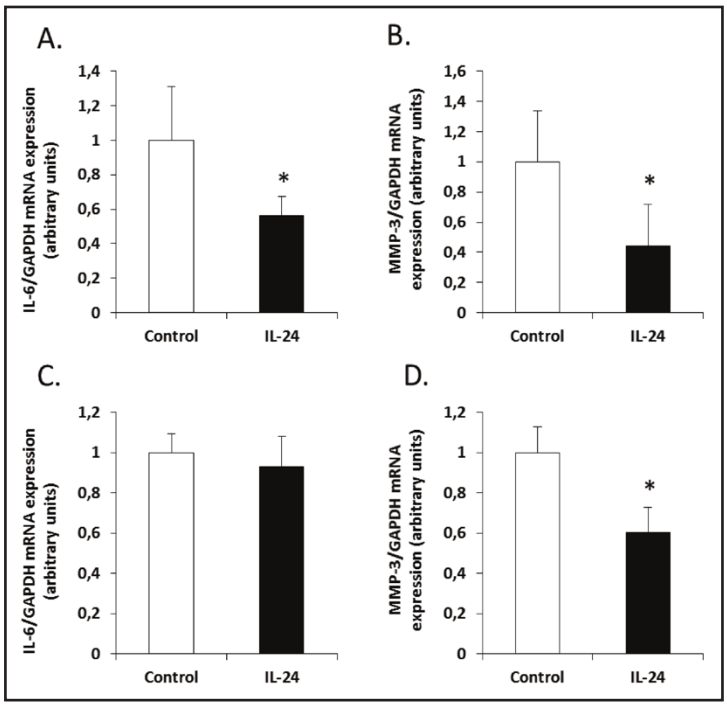

Fig. 9. Effect of interleukin (IL)-24 on the mRNA expression of interleukin (IL)-6 (A, C) and matrix metalloproteinase (MMP)-3 (B, D) in HEK-293 embryonic kidney cells (A, B) and HK2 human renal tubular epithelial cells (C, D). Results are presented as mean+SD. *$p<0.05$ vs. Control.

Discussion

In the present study our purpose was to identify novel genes and pathways involved in the pathomechanism of CON. CON is the leading cause of pediatric CKD accompanied by diminished renal function [20]. The severity of congenital developmental anomalies of the urinary tract can vary from the subclinical mild or temporary stenosis to complete obstruction. While mild stenosis do not lead to serious clinical consequences sever urinary tract obstruction results in CON [21, 22]. The high morbidity and mortality rate of pediatric patients with CON and the limitations of currently available treatment options emphasize

the need to better understand the underlying mechanisms [23]. In the present study we used a neonatal rat model of complete UUO. The early postnatal period of rats corresponds to the midgestation phase of humans [24] therefore it is an appropriate model to study the effect of developmental disorders on the progression of CON and the underlying molecular mechanisms.

Our genome-wide analysis performed on newborn rat kidneys revealed 880 differentially expressed genes following complete UUO. Enrichment analysis of these genes resulted in GO terms (Supplemental Table 2.-4.) and molecular pathways (Supplemental Table 5.) associated mainly with the immune homeostasis, which confirms that developmental abnormalities trigger chronic renal inflammation leading to the excessive deposition of ECM components and consequent renal fibrosis [22].

In the present study we found that 3 of the 10 most upregulated genes, including MMP-3, MMP-7 and MMP-12 are members of the family of MMPs. So far 25 members of the MMP family are known and through their ability to cleave collagens, elastin and other ECM components they play essential role in tissue remodeling [25]. However the biological function of MMP-12, also known as macrophage metalloelastase is less studied. Although, its involvement in the pathomechanism of neonatal UUO has been completely unknown. In accordance with to our present findings, increased mRNA expression of MMP-12 was shown in the kidneys of adult mice after 7 days of UUO and also in the kidney of PKD/Mhm rats which are used to study the molecular mechanism of human autosomal polycystic kidney disease [26-28]. To the best of our knowledge, so far there has been only one study carried out by Abraham *et al.,* which investigated the role of MMP-12 in mice model of UUO induced renal fibrosis (25). Using MMP-12 KO mice they observed that MMP-12 gene deficiency does not alter the relative area of αSMA or collagen deposits in the obstructed kidney suggesting that MMP12 does not play an essential role in the development of renal fibrosis. However in contrast to the observations of Abraham *et al*. Churg *et al*. demonstrated that MMP-12 play a central role in the cigarette smoke-induced lung inflammation and connective tissue breakdown [29, 30]. Moreover, Pellicoro *et al*. observed enhanced MMP-12-induced degradation of elastin in an experimental model of liver fibrosis suggesting its crucial role in ECM remodeling [31].

To clarify the contradiction, in the present study to clarify the contradictions we investigated the role of the well-known determinative molecules of organ fibrosis on the synthesis of MMP12. Previously, it has been demonstrated that TGF-β [32-34], PDGF-B [35] or oxidative stress [36, 37] play a central role in the activation of renal fibroblasts and also in the regulation of the synthesis of MMPs including MMP-1, MMP-2, MMP-9 and MMP-10 [38-42]. Our in vitro experiments demonstrated that while rhPDGF-B treatment or oxidative stress increased the expression of MMP-12 of HEK-293 or HK-2 cells, treatment with rhTGF-β, the strongest known inducer of ECM deposition inhibited its synthesis. Taken together, based on our *in vivo* and *in vitro* experiments and the previous observations demonstrating that MMP-12 can effectively degrade the components of ECM it is easily acceptable that during the early phase of fibrosis when the remodeling of ECM is in the foreground of the process, MMP12 actively participate in the degradation of the ECM components. However, later when tissue remodeling is shifted towards the TGF-β-driven increased deposition of ECM, the synthesis of MMP-12 is decreased, thus facilitating further accumulation of the scar tissue.

In addition to the results discussed above, the expression of IL-24 a member of the IL-20 subfamily, belonging to the grater IL-10 family of cytokines, was also significantly elevated in the kidney of neonate rats following UUO. IL-20 subfamily of cytokines are mainly produced by immune cells and classified into the subfamily based on their common receptor heterodimers (IL22RA1 or IL-20RA/IL-10RB or IL-20RB) and similarities in their target cell specificity [43, 44]. Importance of the IL-20 subfamily of cytokines has been proposed in different chronic inflammatory diseases. Indeed, members of the IL-20 subfamily have been suggested to facilitate the communication between the immune system and epithelial cells thereby enhancing innate defense mechanisms [45]. To date, most experiments have focused

on IL-22, making it the best characterized member of the IL-20 subfamily. However, elevated urinary protein level of IL-19 was shown in adult patients with stage-5 CKD [46], and its increased renal expression was observed in the mouse model of ischaemia-reperfusion-induced acute kidney injury[47]. Involvement of IL-20 subfamily in the pathomechanism of CON is less known.

To the best of our knowledge this is the first study demonstrating the increased mRNA expression and protein level of IL-24 in relation to tissue remodeling of the kidney. Recently, in accordance with our findings increased expression of IL-24 was observed in the edge of cutaneous rat wounds [48]. Furthermore, adenoviral overexpression of IL-24 was demonstrated to suppress the proliferation of fibroblasts isolated from human keloids [49] suggesting the role of IL-24 in tissue remodeling and/or fibrosis. Interestingly, in the present study we found that rhTGF-β, rhPDGF-B or H_2O_2 may inhibit or do not alter the synthesis of IL-24 suggesting rather a negative correlation between IL-24 and the main profibrotic factors. Previously, in congruence with our findings Reinhold D *et al.* found that TGF-β1 inhibits interleukin-10 production in pokeweed mitogen-stimulated peripheral blood mononuclear cells and T cells [50].

Finally, investigating the possible biological role of IL-24 we have demonstrated that rhIL-24 treatment downregulates the mRNA expression of MMP3 - which was identified as the most upregulated gene in our animal model of CON - in HEK-293 and HK-2 cells. Moreover, rhIL-24 also decreased the mRNA expression of pro-inflammatory cytokine IL-6 in the HEK-293 cells. Considering that IL-24 is a member of the family of IL-10 cytokines our results might not be so surprising. Indeed, it has been demonstrated that IL-10 deficiency aggravates kidney inflammation and fibrosis in the mouse model of unilateral ureteral obstruction [51]. Additionally, Semedo *et al.* and Donizetti *et al.* found that IL-10 expression was negatively correlated with the expression of fibrotic genes in remnant kidney model and unilateral ischemia model [52, 53]. Studies in other organs, including lung, heart, pancreas and liver, also showed IL-10 can suppress inflammatory response and thereby inhibit matrix remodeling and fibrosis, even if fibrosis had already developed [54-60].

Taken together, the above mentioned literary data and our results suggest that similarly to other members of the IL-10 family of cytokines IL-24 may have anti-inflamatory properties.

Conclusion

In summary, our data provide a bioinformatic analysis of differentially expressed genes and molecular pathways potentially involved in the pathophysiology of CON, thus contributing to the better understanding of the underlying molecular mechanisms. The differentially expressed genes including MMP-3, MMP-7 and MMP-12, IL-19 and -24 have the potential to be used as targets for early diagnosis and treatment of CON. Our data suggest that IL-24 plays a role in the pathophysiology of CON via regulation of immune response and tissue remodeling.

Disclosure Statement

The authors declare no competing interests.

Acknowledgments

We are grateful to Maria Bernáth for her excellent technical assistance. This work was supported by Hungarian National Scientific Research Foundation Grant - OTKA K116928, K108688, NN114607, PD105361 and LP008/2016.

References

1 Chevalier RL, Thornhill BA, Forbes MS, Kiley SC: Mechanisms of renal injury and progression of renal disease in congenital obstructive nephropathy. Pediatr Nephrol 2010;25:687-697.

2 Klein J, Gonzalez J, Miravete M, Caubet C, Chaaya R, Decramer S, Bandin F, Bascands JL, Buffin-Meyer B, Schanstra JP: Congenital ureteropelvic junction obstruction: human disease and animal models. Int J Exp Pathol 2011;92:168-192.

3 Silverstein DM, Travis BR, Thornhill BA, Schurr JS, Kolls JK, Leung JC, Chevalier RL: Altered expression of immune modulator and structural genes in neonatal unilateral ureteral obstruction. Kidney Int 2003;64:25-35.

4 Haugen E, Nath KA: The involvement of oxidative stress in the progression of renal injury. Blood Purif 1999;17:58-65.

5 Qin J, Mei WJ, Xie YY, Huang L, Yuan QJ, Hu GY, Tao LJ, Peng ZZ: Fluorofenidone attenuates oxidative stress and renal fibrosis in obstructive nephropathy via blocking NOX2 (gp91phox) expression and inhibiting ERK/MAPK signaling pathway. Kidney Blood Press Res 2015;40:89-99.

6 Kaneto H, Morrissey J, Klahr S: Increased expression of TGF-beta 1 mRNA in the obstructed kidney of rats with unilateral ureteral ligation. Kidney Int 1993;44:313-321.

7 Nguyen HT, Thomson AA, Kogan BA, Baskin LS, Cunha GR: Growth factor expression in the obstructed developing and mature rat kidney. Lab Invest 1999;79:171-184.

8 Vianna HR, Soares CM, Tavares MS, Teixeira MM, Silva AC: [Inflammation in chronic kidney disease: the role of cytokines]. J Bras Nefrol 2011;33:351-364.

9 Pedroza M, Schneider DJ, Karmouty-Quintana H, Coote J, Shaw S, Corrigan R, Molina JG, Alcorn JL, Galas D, Gelinas R, Blackburn MR: Interleukin-6 contributes to inflammation and remodeling in a model of adenosine mediated lung injury. PLoS One 2011;6:e22667.

10 Liu Y: Cellular and molecular mechanisms of renal fibrosis. Nat Rev Nephrol 2011;7:684-696.

11 Wuhl E, Schaefer F: Therapeutic strategies to slow chronic kidney disease progression. Pediatr Nephrol 2008;23:705-716.

12 Hermida RC, Smolensky MH, Ayala DE, Portaluppi F: Ambulatory Blood Pressure Monitoring (ABPM) as the reference standard for diagnosis of hypertension and assessment of vascular risk in adults. Chronobiol Int 2015;32:1329-1342.

13 Galarreta CI, Thornhill BA, Forbes MS, Simpkins LN, Kim DK, Chevalier RL: Transforming growth factor-beta1 receptor inhibition preserves glomerulotubular integrity during ureteral obstruction in adults but worsens injury in neonatal mice. Am J Physiol Renal Physiol 2013;304:F481-490.

14 Tolgyesi G, Molnar V, Semsei AF, Kiszel P, Ungvari I, Pocza P, Wiener Z, Komlosi ZI, Kunos L, Galffy G, Losonczy G, Seres I, Falus A, Szalai C: Gene expression profiling of experimental asthma reveals a possible role of paraoxonase-1 in the disease. Int Immunol 2009;21:967-975.

15 Zhang Y, Wang J, Huang S, Zhu X, Liu J, Yang N, Song D, Wu R, Deng W, Skogerbo G, Wang XJ, Chen R, Zhu D: Systematic identification and characterization of chicken (Gallus gallus) ncRNAs. Nucleic Acids Res 2009;37:6562-6574.

16 Gene Ontology C: Gene Ontology Consortium: going forward. Nucleic Acids Res 2015;43:D1049-1056.

17 Croft D, Mundo AF, Haw R, Milacic M, Weiser J, Wu G, Caudy M, Garapati P, Gillespie M, Kamdar MR, Jassal B, Jupe S, Matthews L, May B, Palatnik S, Rothfels K, Shamovsky V, Song H, Williams M, Birney E, Hermjakob H, Stein L, D'Eustachio P: The Reactome pathway knowledgebase. Nucleic Acids Res 2014;42:D472-477.

18 Vilella AJ, Severin J, Ureta-Vidal A, Heng L, Durbin R, Birney E: EnsemblCompara GeneTrees: Complete, duplication-aware phylogenetic trees in vertebrates. Genome Res 2009;19:327-335.

19 Shannon P, Markiel A, Ozier O, Baliga NS, Wang JT, Ramage D, Amin N, Schwikowski B, Ideker T: Cytoscape: a software environment for integrated models of biomolecular interaction networks. Genome Res 2003;13:2498-2504.

20 Chevalier RL, Forbes MS, Galarreta CI, Thornhill BA: Responses of proximal tubular cells to injury in congenital renal disease: fight or flight. Pediatr Nephrol 2014;29:537-541.

21 Thornhill BA, Burt LE, Chen C, Forbes MS, Chevalier RL: Variable chronic partial ureteral obstruction in the neonatal rat: a new model of ureteropelvic junction obstruction. Kidney Int 2005;67:42-52.

22 Ingraham SE, McHugh KM: Current perspectives on congenital obstructive nephropathy. Pediatr Nephrol 2011;26:1453-1461.
23 Haider DG, Sauter T, Lindner G, Masghati S, Peric S, Friedl A, Wolzt M, Horl WH, Soleiman A, Exadaktylos A, Fuhrmann V: Use of Calcium Channel Blockers is Associated with Mortality in Patients with Chronic Kidney Disease. Kidney Blood Press Res 2015;40:630-637.
24 Merlet-Benichou C, Gilbert T, Muffat-Joly M, Lelievre-Pegorier M, Leroy B: Intrauterine growth retardation leads to a permanent nephron deficit in the rat. Pediatr Nephrol 1994;8:175-180.
25 Giannandrea M, Parks WC: Diverse functions of matrix metalloproteinases during fibrosis. Dis Model Mech 2014;7:193-203.
26 Abraham AP, Ma FY, Mulley WR, Ozols E, Nikolic-Paterson DJ: Macrophage infiltration and renal damage are independent of matrix metalloproteinase 12 in the obstructed kidney. Nephrology (Carlton) 2012;17:322-329.
27 Summers SA, Gan PY, Dewage L, Ma FT, Ooi JD, O'Sullivan KM, Nikolic-Paterson DJ, Kitching AR, Holdsworth SR: Mast cell activation and degranulation promotes renal fibrosis in experimental unilateral ureteric obstruction. Kidney Int 2012;82:676-685.
28 Dweep H, Sticht C, Kharkar A, Pandey P, Gretz N: Parallel analysis of mRNA and microRNA microarray profiles to explore functional regulatory patterns in polycystic kidney disease: using PKD/Mhm rat model. PLoS One 2013;8:e53780.
29 Churg A, Wang RD, Tai H, Wang X, Xie C, Dai J, Shapiro SD, Wright JL: Macrophage metalloelastase mediates acute cigarette smoke-induced inflammation via tumor necrosis factor-alpha release. Am J Respir Crit Care Med 2003;167:1083-1089.
30 Churg A, Zay K, Shay S, Xie C, Shapiro SD, Hendricks R, Wright JL: Acute cigarette smoke-induced connective tissue breakdown requires both neutrophils and macrophage metalloelastase in mice. Am J Respir Cell Mol Biol 2002;27:368-374.
31 Pellicoro A, Aucott RL, Ramachandran P, Robson AJ, Fallowfield JA, Snowdon VK, Hartland SN, Vernon M, Duffield JS, Benyon RC, Forbes SJ, Iredale JP: Elastin accumulation is regulated at the level of degradation by macrophage metalloelastase (MMP-12) during experimental liver fibrosis. Hepatology 2012;55:1965-1975.
32 Pilmore HL, Yan Y, Eris JM, Hennessy A, McCaughan GW, Bishop GA: Time course of upregulation of fibrogenic growth factors and cellular infiltration in a rodent model of chronic renal allograft rejection. Transpl Immunol 2002;10:245-254.
33 Bottinger EP, Bitzer M: TGF-beta signaling in renal disease. J Am Soc Nephrol 2002;13:2600-2610.
34 Fukuda N, Tahira Y, Matsuda H, Matsumoto K: Transforming growth factor-beta as a treatment target in renal diseases. J Nephrol 2009;22:708-715.
35 Chen YT, Chang FC, Wu CF, Chou YH, Hsu HL, Chiang WC, Shen J, Chen YM, Wu KD, Tsai TJ, Duffield JS, Lin SL: Platelet-derived growth factor receptor signaling activates pericyte-myofibroblast transition in obstructive and post-ischemic kidney fibrosis. Kidney Int 2011;80:1170-1181.
36 Kim J, Seok YM, Jung KJ, Park KM: Reactive oxygen species/oxidative stress contributes to progression of kidney fibrosis following transient ischemic injury in mice. Am J Physiol Renal Physiol 2009;297:F461-470.
37 Nelson KK, Melendez JA: Mitochondrial redox control of matrix metalloproteinases. Free Radic Biol Med 2004;37:768-784.
38 Asano K, Shikama Y, Shoji N, Hirano K, Suzaki H, Nakajima H: Tiotropium bromide inhibits TGF-beta-induced MMP production from lung fibroblasts by interfering with Smad and MAPK pathways in vitro. Int J Chron Obstruct Pulmon Dis 2010;5:277-286.
39 Kim ES, Sohn YW, Moon A: TGF-beta-induced transcriptional activation of MMP-2 is mediated by activating transcription factor (ATF)2 in human breast epithelial cells. Cancer Lett 2007;252:147-156.
40 Behzadian MA, Wang XL, Windsor LJ, Ghaly N, Caldwell RB: TGF-beta increases retinal endothelial cell permeability by increasing MMP-9: possible role of glial cells in endothelial barrier function. Invest Ophthalmol Vis Sci 2001;42:853-859.
41 Ishikawa F, Miyoshi H, Nose K, Shibanuma M: Transcriptional induction of MMP-10 by TGF-beta, mediated by activation of MEF2A and downregulation of class IIa HDACs. Oncogene 2010;29:909-919.

42 Ito I, Fixman ED, Asai K, Yoshida M, Gounni AS, Martin JG, Hamid Q: Platelet-derived growth factor and transforming growth factor-beta modulate the expression of matrix metalloproteinases and migratory function of human airway smooth muscle cells. Clin Exp Allergy 2009;39:1370-1380.
43 Conti P, Kempuraj D, Frydas S, Kandere K, Boucher W, Letourneau R, Madhappan B, Sagimoto K, Christodoulou S, Theoharides TC: IL-10 subfamily members: IL-19, IL-20, IL-22, IL-24 and IL-26. Immunol Lett 2003;88:171-174.
44 Sziksz E, Pap D, Lippai R, Beres NJ, Fekete A, Szabo AJ, Vannay A: Fibrosis Related Inflammatory Mediators: Role of the IL-10 Cytokine Family. Mediators Inflamm 2015;2015:764641.
45 Rutz S, Wang X, Ouyang W: The IL-20 subfamily of cytokines--from host defence to tissue homeostasis. Nat Rev Immunol 2014;14:783-795.
46 Jennings P, Crean D, Aschauer L, Limonciel A, Moenks K, Kern G, Hewitt P, Lhotta K, Lukas A, Wilmes A, Leonard MO: Interleukin-19 as a translational indicator of renal injury. Arch Toxicol 2015;89:101-106.
47 Hsu YH, Li HH, Sung JM, Chen WT, Hou YC, Chang MS: Interleukin-19 mediates tissue damage in murine ischemic acute kidney injury. PLoS One 2013;8:e56028.
48 Soo C, Shaw WW, Freymiller E, Longaker MT, Bertolami CN, Chiu R, Tieu A, Ting K: Cutaneous rat wounds express c49a, a novel gene with homology to the human melanoma differentiation associated gene, mda-7. J Cell Biochem 1999;74:1-10.
49 Liang J, Huang RL, Huang Q, Peng Z, Zhang PH, Wu ZX: Adenovirus-mediated human interleukin 24 (MDA-7/IL-24) selectively suppresses proliferation and induces apoptosis in keloid fibroblasts. Ann Plast Surg 2011;66:660-666.
50 Reinhold D, Bank U, Buhling F, Lendeckel U, Ansorge S: Transforming growth factor beta 1 inhibits interleukin-10 mRNA expression and production in pokeweed mitogen-stimulated peripheral blood mononuclear cells and T cells. J Interferon Cytokine Res 1995;15:685-690.
51 Jin Y, Liu R, Xie J, Xiong H, He JC, Chen N: Interleukin-10 deficiency aggravates kidney inflammation and fibrosis in the unilateral ureteral obstruction mouse model. Lab Invest 2013;93:801-811.
52 Semedo P, Correa-Costa M, Antonio Cenedeze M, Maria Avancini Costa Malheiros D, Antonia dos Reis M, Shimizu MH, Seguro AC, Pacheco-Silva A, Saraiva Camara NO: Mesenchymal stem cells attenuate renal fibrosis through immune modulation and remodeling properties in a rat remnant kidney model. Stem Cells 2009;27:3063-3073.
53 Donizetti-Oliveira C, Semedo P, Burgos-Silva M, Cenedeze MA, Malheiros DM, Reis MA, Pacheco-Silva A, Camara NO: Adipose tissue-derived stem cell treatment prevents renal disease progression. Cell Transplant 2012;21:1727-1741.
54 Huang YH, Shi MN, Zheng WD, Zhang LJ, Chen ZX, Wang XZ: Therapeutic effect of interleukin-10 on CCl4-induced hepatic fibrosis in rats. World J Gastroenterol 2006;12:1386-1391.
55 Demols A, Van Laethem JL, Quertinmont E, Degraef C, Delhaye M, Geerts A, Deviere J: Endogenous interleukin-10 modulates fibrosis and regeneration in experimental chronic pancreatitis. Am J Physiol Gastrointest Liver Physiol 2002;282:G1105-1112.
56 Van Laethem JL, Eskinazi R, Louis H, Rickaert F, Robberecht P, Deviere J: Multisystemic production of interleukin 10 limits the severity of acute pancreatitis in mice. Gut 1998;43:408-413.
57 Garantziotis S, Brass DM, Savov J, Hollingsworth JW, McElvania-TeKippe E, Berman K, Walker JK, Schwartz DA: Leukocyte-derived IL-10 reduces subepithelial fibrosis associated with chronically inhaled endotoxin. Am J Respir Cell Mol Biol 2006;35:662-667.
58 Nakagome K, Dohi M, Okunishi K, Tanaka R, Miyazaki J, Yamamoto K: In vivo IL-10 gene delivery attenuates bleomycin induced pulmonary fibrosis by inhibiting the production and activation of TGF-beta in the lung. Thorax 2006;61:886-894.
59 Krishnamurthy P, Rajasingh J, Lambers E, Qin G, Losordo DW, Kishore R: IL-10 inhibits inflammation and attenuates left ventricular remodeling after myocardial infarction via activation of STAT3 and suppression of HuR. Circ Res 2009;104:e9-18.
60 Apparailly F, Verwaerde C, Jacquet C, Auriault C, Sany J, Jorgensen C: Adenovirus-mediated transfer of viral IL-10 gene inhibits murine collagen-induced arthritis. J Immunol 1998;160:5213-5220.